The Astrophysical Journal, 675:868–874, 2008 March 1

FIELD LINE SHRINKAGE IN FLARES OBSERVED BY THE X-RAY TELESCOPE ON *HINODE*

Katharine K. Reeves
Harvard-Smithsonian Center for Astrophysics, 60 Garden Street MS 58, Cambridge, MA 02138; kreeves@cfa.harvard.edu
and
Daniel B. Seaton and Terry G. Forbes
Institute for the Study of Earth, Oceans, and Space (EOS), University of New Hampshire, 39 College Road, Durham, NH 03824; dseaton@unh.edu, terry.forbes@unh.edu
Received 2007 July 24; accepted 2007 November 8

ABSTRACT

The X-Ray Telescope on *Hinode* has observed individual loops of plasma moving downward in a manner that is consistent with field line shrinkage in the aftermath of reconnection at higher altitudes. An on-disk B3.8 flare observed on 2007 May 2 has loops that clearly change in shape from cusp-shaped to more rounded. In addition, bright loops are observed that decrease in altitude with a speed of approximately 5 km s^{-1}, and fainter, higher loop structures shrink with a velocity of 48 km s^{-1}. A C2.1 flare observed on 2006 December 17 also has loops that change shape. Many bright features are seen to be moving downward in this event, and we estimate their speed to be around 2–4 km s^{-1}. We measure the shrinkage in both of these events, and find that it is 17%–27%, which is consistent with theoretical predictions.

Subject headings: Sun: flares — Sun: X-rays, gamma rays

1. INTRODUCTION

Magnetic reconnection is thought to be the dominant process responsible for solar flares. In the standard model of flare reconnection, open magnetic field lines are swept through a current sheet, reconnecting with each other to form cusp-shaped loops in the corona. These cusp-shaped loops should then relax into a more potential, rounded state (Priest & Forbes 2002). This phenomenon is often referred to as field line shrinkage (Švestka et al. 1987). Using a Kopp-Pneuman-type magnetic configuration, Lin (2004) calculated that this shrinkage happens faster just after the loop is reconnected, and that loops reconnected early in an event undergo more shrinkage than those that reconnect later. Lin et al. (1995) found that for two-dimensional models the loops can shrink dramatically in the early phase of a flare, losing most of their original height. In the late phase of a flare, these calculations predict that loops shrink less, and that they lose on the order of 20% of their original height.

There have been several indirect observations of field line shrinkage. Švestka et al. (1987) found that hot X-ray loops were positioned above cooler loops seen in Hα observations, and that the Hα loops never reached the heights of the X-ray loops. This observation indicated that the flare loops had undergone shrinkage as they cooled. A similar result was obtained by Vršnak et al. (2006), who followed height versus time curves from different instruments for a flare, and discovered that the same features found in the high-temperature instruments were repeated in the lower temperature instruments, but at a lower height. Forbes & Acton (1996) inferred field line shrinkage from the change in shape of intensity features in some flares observed with the Soft X-ray Telescope (SXT) on *Yohkoh*. They found that the field lines shrink to about 20% of their initial height in one case and 35% in another. Hiei & Hundhausen (1996) observed a large coronal arch with SXT, and found that bright features at the tops of the loops making up the arch shrank with a velocity of around 2–3 km s^{-1}.

High-energy sources observed in flares using the *Reuven Ramaty High-Energy Solar Spectroscopic Imager* (*RHESSI*) have also shown downward motion that has been interpreted as field line shrinkage. Flares observed by Sui & Holman (2003) and Sui et al. (2004) had sources at 6–12 keV that moved downward at 8–15 km s^{-1} and 12–25 keV sources that moved downward at 11–23 km s^{-1}. Veronig et al. (2006) observed an X3.9 flare with *RHESSI* and found that the speed of the downward motion increased at higher energies. These observations are consistent with the theoretical picture put forth by Lin (2004), since they indicate that the hotter sources (which are higher in altitude) move downward faster.

The X-Ray Telescope (XRT) on *Hinode*, with its high spatial and temporal resolution, gives an unprecedented view of the morphology of flare loops. In this paper we present evidence for field line shrinkage in two flares observed by XRT. The observations are described in § 2; in § 3 we give our results and discussion, and our conclusions are presented in § 4.

2. OBSERVATIONS

The XRT on the *Hinode* satellite is a modified Wolter I grazing incidence imaging telescope with a 35 cm aperture and a 2.71 m focal length (Golub et al. 2007). It has two filter wheels in the focal plane with a total of nine X-ray filters. The CCD on XRT is 2048×2048 pixels, and each pixel is approximately 1″ (Kano et al. 2008).

For this paper, we examine two flares observed by XRT: a B3.8 flare that began at 18:05 UT on 2007 May 2 and a C2.1 flare that began at 14:47 UT on 2006 December 17. Both of these events were relatively long-duration events (see *GOES* plots in Figs. 2 and 4). The B flare was observed using the titanium/polyamide filter with an approximate cadence of 15 s. The C flare was observed using the aluminum/polyamide filter with a cadence of about 2 minutes. The two filters used in these observations both have broad temperature coverage peaking at around 6–10 MK.

3. RESULTS AND DISCUSSION

Figure 1 shows a diagram of reconnecting loops, illustrating the shrinkage that should occur after reconnection, according to

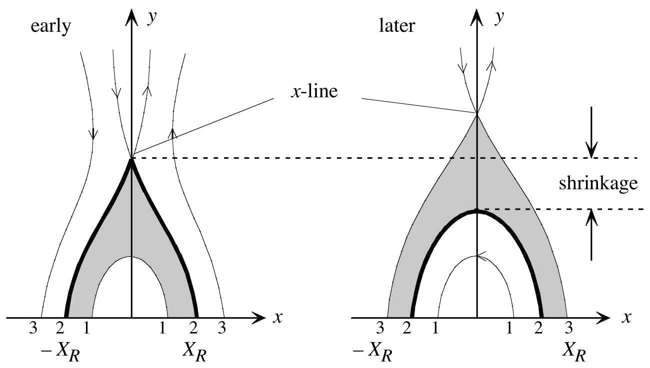

FIG. 1.—Field lines change from a cusp shape immediately following reconnection (*left*) to a more rounded shape at a later time (*right*) (figure reproduced courtesy of ASP Conf. Ser. from Forbes 1997).

theoretical models. When the field line is first reconnected, as shown in Figure 1 (*left*), the field line is connected to the X-point and has a cusp shape at the top. As time progresses, the loop disconnects from the X-point and relaxes to a more potential configuration, taking on a more rounded shape, as shown in Figure 1 (*right*). During this process, the footpoints of the loop are line-tied in the chromosphere, so that the footpoint ends of the loop do not move.

In this paper, we use two methods to study the apparent shrinking motion of the flare loops observed by the XRT. The first method was developed by Forbes & Acton (1996), and it determines the percentage of shrinkage of the postflare loops by comparing the altitudes of loop tops at different times. This method provides only an average value of how much a field line shrinks as it "moves" through the visible flare loop structure. In the second method, we extract a strip of the XRT image that intersects the flare loops and plot the changes in intensity in this strip as a function of time. This procedure provides a much more stringent test of shrinkage models if individual field lines can be identified and tracked within the flare loop system. At any given time, each field line will undergo a different rate of shrinkage depending on its position relative to the cusp point at the lower tip of the current sheet. Following several fields lines, therefore, provides a measure of shrinkage as a function of time and space rather than just a single average value.

Figure 2 shows a C2.1 flare observed on 2006 December 17. The images in the top row show the flare at two different times, and they have been edge-enhanced using the Sobel filter. The panel in the bottom left shows contours from each of these images overlaid. The crosses on the contours show the points used to calculate the altitude of the shrinking loops, as described below. There is some distortion in the inner edge of the contour at

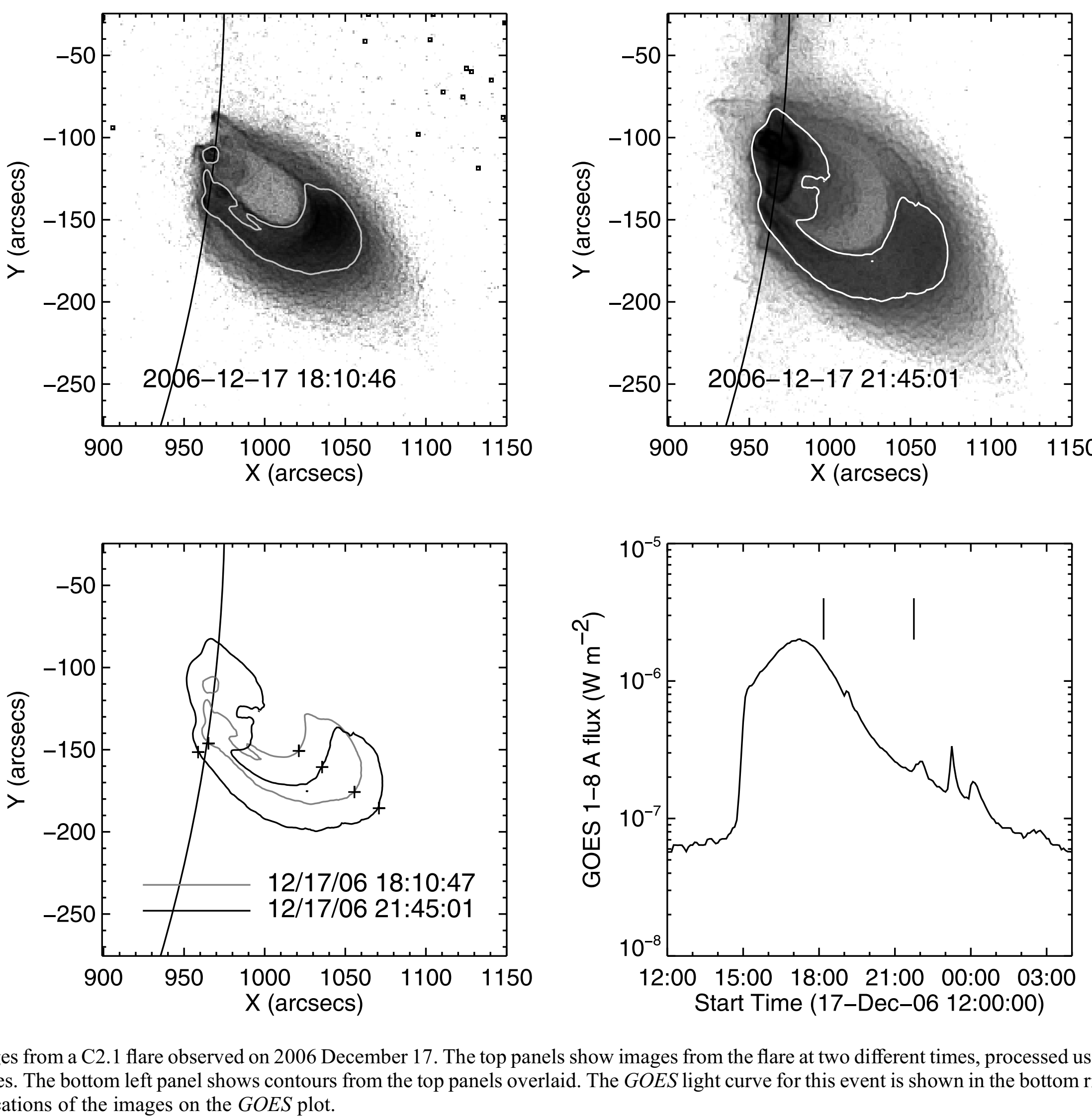

FIG. 2.—Images from a C2.1 flare observed on 2006 December 17. The top panels show images from the flare at two different times, processed using a Sobel filter to bring out the edges. The bottom left panel shows contours from the top panels overlaid. The *GOES* light curve for this event is shown in the bottom right panel. Vertical bars mark the locations of the images on the *GOES* plot.

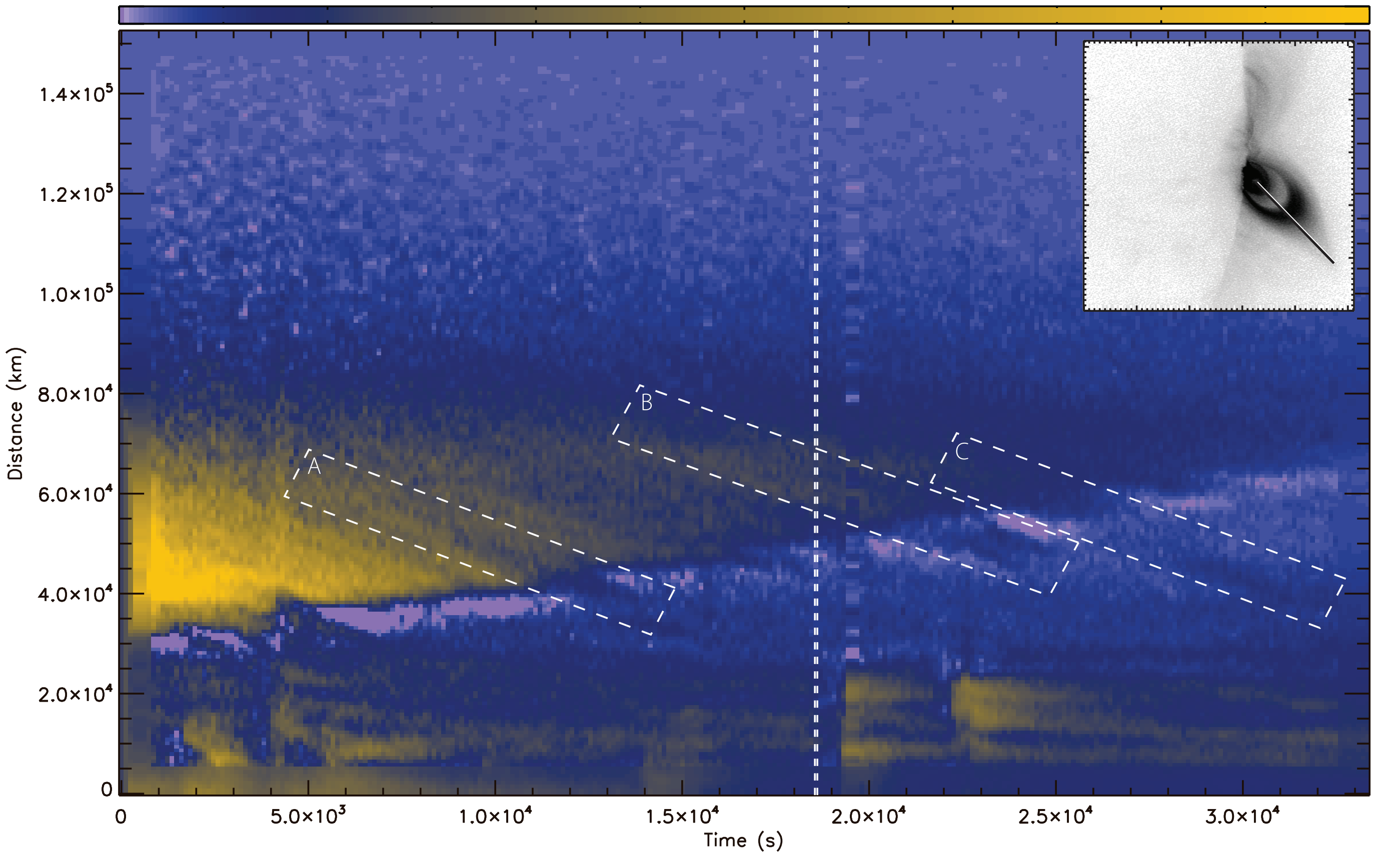

FIG. 3.—Plot of the intensity along a five-pixel slice from pixel (328, 241) to (475, 89) as a function of time, starting at 2006 December 17, 18:00:53 UT. The data have been processed using a low-pass filter to remove noise, and a Sobel filter and unsharp mask have been applied to enhance the edges. Boxes indicate the locations of some of the bright features that shrink with time. The location of the slice on the flare image is shown in the inset in the upper right corner.

the later time due to other loop structures that appear near the Sun's limb, but careful examination of Figure 2 (*top right*) shows that the inner leg of the loop extends in a straight line from the point at which the contour deviates to the surface of the Sun.

We follow the method of Forbes & Acton (1996) to measure the shrinkage in the loops. In order to make certain that we are looking at the same set of loops at earlier and later times, we choose loop system contours whose outer edge at the earlier time lines up reasonably well with the inner edge of the loop system contour at the later time. This process is equivalent to lining up the contours of the gray-shaded areas of the two configurations in Figure 1. Since the footpoint of the loop is line-tied to the chromosphere, the inner edge of the contour at the later time should line up with the outer edge of the contour at the earlier time.

Forbes & Acton (1996) calculate that the shrinkage of a loop system is given by

$$s = \frac{y_{o1}(x) - y_{i2}(x)}{y_{o1}(x)}, \quad (1)$$

where y_{o1} is the height of the outer edge of the loop at the earlier time, y_{i2} is the height of the inner edge of the loop at the later time, and x is the location of the footpoint. Using the points marked with crosses on the contours in Figure 2 (*bottom left*), we find that this loop system has shrunk by approximately 27%. Since this value is measured during the decay phase of the flare (see the *GOES* plot in Fig. 2), it agrees quite well with the predicted values calculated by Lin (2004).

There are many bright looplike structures in this flare that appear to have downward motion as the flare evolves. In order to capture the motion of these features, we plot the intensity along a line from near the solar surface to the cusp of the flare loops as a function of time in Figure 3. To create this image, we apply a low-pass spatial filter to the data to remove the worst of the CCD noise from the images, then apply a Sobel filter and an unsharp mask to enhance the edges. A stack plot is constructed by taking a slice at a fixed location from each image and displaying the set of slices side by side, in order of increasing time. The resulting stack plot is oriented such that the cusp of the flare is near the top of each slice. The location of the slice used to create the stack plot is shown in the inset XRT image in Figure 3.

In Figure 3, several features are evident. There is an upward-sloping line where the intensity gets low in the XRT image on the inner edge of the flare loop system. This edge is a cooling front that rises as new loops are reconnected into the arcade and cool. The response function of the aluminum/polyamide filter is not very sensitive to plasma at 1 MK and below, so as soon as the loops cool past that threshold, they are no longer seen in the XRT.

In addition to this feature, many small-scale downward-sloping features are also visible in Figure 3. These features are due to downward-moving intensity enhancements in the flare loop system. Some of the prominent ones are outlined in the figure with boxes marked A, B, and C. We measure the velocities of these features by calculating their slopes in Figure 3 and find that they move with velocities of approximately 2–4 km s^{-1}. Observations by the *Transition Region and Coronal Explorer* (*TRACE*) of the same region in the 195 Å passband show loops forming and shrinking slightly with the same velocity as these small-scale features. Since these loops appear just below the XRT intensity enhancements that created these downward-sloping features, we conclude

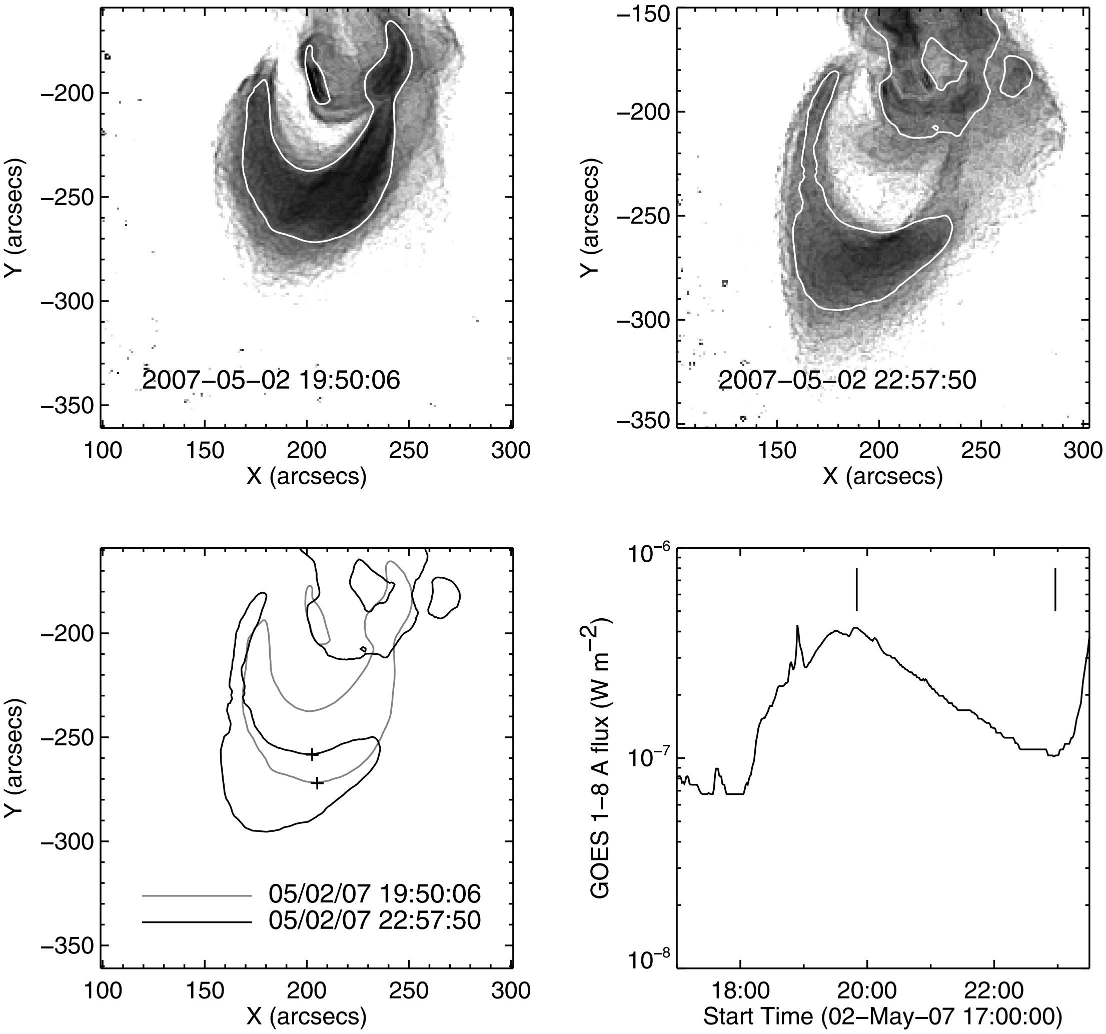

Fig. 4.—Images from a B3.8 flare observed on 2007 May 5. The top panels show images from the flare at two different times, processed using a Sobel filter to bring out the edges. The bottom left panel shows contours from the top panels overlaid. The *GOES* light curve for this event is shown in the bottom right panel. Vertical bars mark the locations of the images on the *GOES* plot.

that we are seeing the same loops in both instruments as they cool out of the XRT passband and into the *TRACE* passband. Because they also eventually cool out of the *TRACE* and XRT passbands altogether, we see only a brief snapshot of their motion, and cannot follow their trajectories as they continue to shrink.

It is interesting that these loops continue to be bright below the cooling front we see in the XRT observations (i.e., they cross the upward-sloping line in Fig. 3). One possible explanation for this behavior is that these loops are cooling more slowly than the average cooling time of the arcade as a whole. This would happen if they were more dense, on average, than the other surrounding loops.

There is no direct evidence for faster motion of loops closer to the cusp region in this event. The plasma in the cusp region is very diffuse in this flare, and individual loops are difficult to make out in this region. Thus the trajectories of the loops as they are first formed (where we would expect to see this more rapid shrinkage) are difficult to determine, and we cannot draw a conclusion about whether they exhibit the characteristic slowing described above. There are ample *RHESSI* data for this flare, and studies are underway to determine if downward motion of *RHESSI* sources can be seen in it, along the lines of those found in Sui & Holman (2003), Sui et al. (2004), and Veronig et al. (2006).

Figure 4 shows the B3.8 flare observed on 2007 May 2. This flare occurred on the disk of the Sun, approximately 200″ west of disk center. As in Figure 2, the top panels in Figure 4 show images of the flare at two different times. These images have been enhanced by applying a Sobel filter to the log-scaled data in order to bring more contrast to the edges. We also present the overlaid contours for these two images in the bottom left panel of Figure 4.

We use the method described above to calculate the shrinkage for this event and find that it is about 17%. This flare shrinks less over a similar time period than the December 17 event. One possible reason for this is that there could be some foreshortening effects in the measurement of the shrinkage in the May 2 event, leading to an underestimate of the shrinkage, as discussed below. Nonetheless, both of the flares studied here exhibit field line shrinkage that is consistent with theoretical predictions.

Figure 5 shows a stack plot for the May 2 event similar to the one shown in Figure 3. In order to improve the contrast of the shrinking loops, which are only a few pixel counts brighter than the diffuse plasma in the background, we construct a background brightness image by calculating the median brightness for each pixel over the course the entire data set. We then subtract this image from each frame of the sequence, removing long-lasting bright structures and leaving only those that vary during the course of the data set, most notably, the shrinking loops. The contrast has been enhanced in the upper right part of the stack plot in order to bring out faint intensity features.

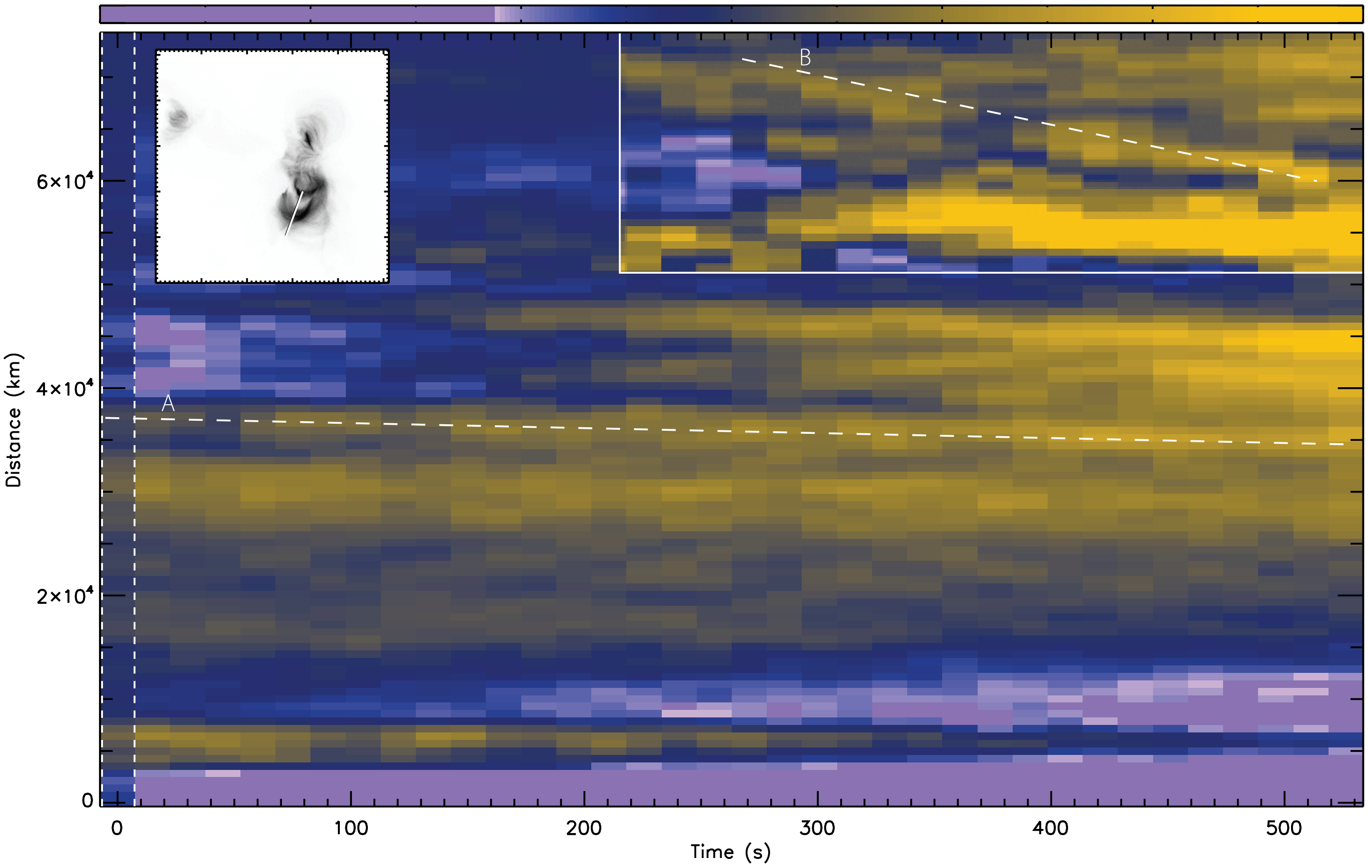

FIG. 5.—Plot of the intensity along a five-pixel slice as a function of time, starting at 2007 May 2, 19:09:16 UT. The data have been processed using a low-pass filter to remove noise, and a Sobel filter and unsharp mask have been applied to enhance the edges. The section of the image in the upper right corner has increased contrast to bring out faint features. Dotted lines indicate the locations of some of the bright features that shrink with time. The location of the slice on the flare image is shown in the inset in the upper left corner.

We have marked two downward-sloping features with dotted lines in Figure 5. The most noticeable, marked with the letter "A", is the bright core loop of the flare. By taking the slope of the dotted line, we find that the velocity of this feature is about 5 km s^{-1}. This feature is well below the cusp of the flare and thus is a mature loop well past the initial reconnection phase. The other feature is marked with a "B", and is higher up in the arcade, near the cusp. These loops are fainter, and when we measure the slope of the line formed by these shrinking features in Figure 5, we find that the velocity of the descending feature is on the order of 48 km s^{-1}. Since these loops are closer to the cusp region, they are closer to the reconnection site, and are at an earlier stage in their evolution than the bright loops in the core of the arcade. They are fainter because, although the temperature of these newly formed loops is high, the emission measure is small, rendering contrast in the observations in this region low. These observations agree well with those of Veronig et al. (2006), who found that more energetic *RHESSI* sources had higher altitudes and larger downward velocities than the less energetic parts of the flare.

Later in the evolution of the flare loops, a compact bright feature appears high in the arcade. Figure 6 (*bottom left*) shows an image taken at 22:56:35 UT. In this image, the compact bright feature appears near the top of the loop. Similar loop top brightenings have been observed at the tops of flare loops in the soft X-rays using the SXT on *Yohkoh* (Tsuneta et al. 1992; McTiernan et al. 1993; Feldman et al. 1994). These bright features are probably condensations caused by either a thermal instability downstream of the termination shock (Forbes & Malherbe 1991) or evaporated material colliding in the loop tops (Reeves et al. 2007). In either case, field line shrinkage would cause bright features such as these to decrease in altitude with time. We follow the motion of the compact bright feature by drawing contours around it and finding its center position by eye. Examples of two images with contours around the bright feature are shown in the top panels of Figure 6. The height of the feature is plotted as a function of time in the bottom right panel of Figure 6.

If we use all of the points plotted in Figure 6 to calculate the velocity of the bright feature, we get a value of approximately 44 km s^{-1}. This value is remarkably similar to the fast-moving but faint feature shown in Figure 5. The motion of the feature is not completely linear, however; its height decreases rapidly for the first 30 s, and then it levels off.

Calculations by Lin (2004) suggest that loops moving due to field line shrinkage should move faster immediately after they are reconnected, and then slow down over time, as shown in Figure 7. The trajectory of the bright feature shown in Figure 6 suggests that this model is correct. The two downward-sloping features in Figure 5 provide additional evidence to support this model, since the lower loop, which is farther away from the reconnection site, is shrinking slowly, while the loops that are higher up, near the cusp region, are shrinking more quickly. In Figure 7, we superimpose the measured trajectories from Figure 5 on top of the model curves, and they fit well with the calculated paths of the loop tops. It should be emphasized, however, that the calculations done by Lin (2004) are not meant to model a specific event, so this juxtaposition should be viewed as a qualitative verification of the model principles, rather than a quantitative comparison.

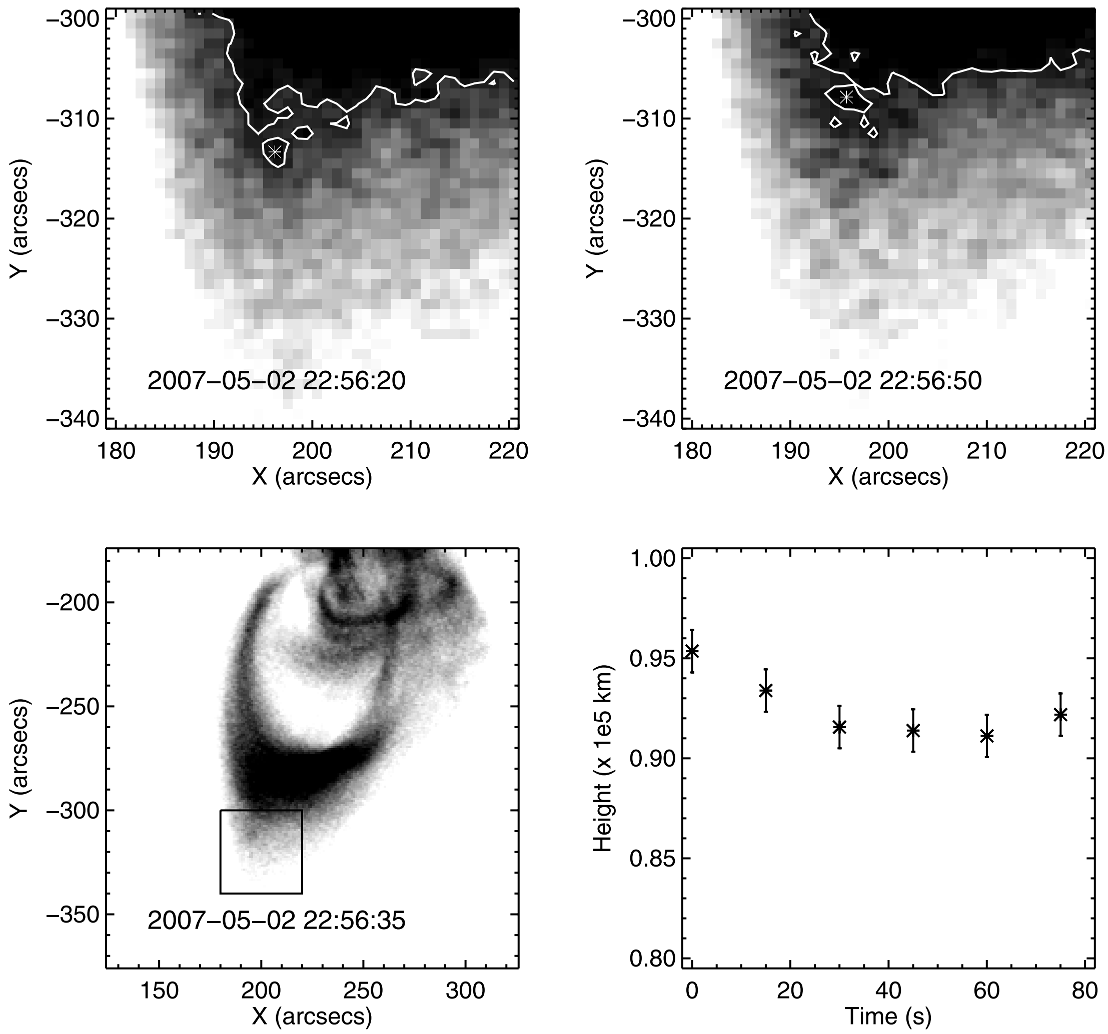

FIG. 6.— *Top*: Contoured images from the B3.8 flare observed on 2007 May 5 used to determine the velocity of the condensation. *Bottom left*: Larger image from the flare, with a box indicating the region plotted in the top panels. *Bottom right*: Plot of the height of the condensation as a function of time. Error bars in this plot are drawn assuming an uncertainty of one pixel in determining the position of the condensation.

Shrinkage has been observed previously in the soft X-rays by Hiei & Hundhausen (1996), who observed downward-moving features in a high-altitude coronal arch system using SXT on *Yohkoh*. They observed bright compact features rather than loops, and it is likely that these compact features were localized condensations on the shrinking field lines. Hiei & Hundhausen (1996) provided no interpretations of their observations—the possibility that they were seeing shrinkage was not discussed in that work—but comparisons of their trajectories with theoretical predictions show that their observations are remarkably consistent with field line shrinkage (Lin 2004). They found that the fastest speed of these features was on the order of 2–3 km s^{-1}, an order of magnitude slower than the fast feature in our observations. However, the event that we are examining evolves at a faster rate, so higher speeds are not unexpected. The event examined by Hiei & Hundhausen (1996) was a large arch that evolved over the course of several days, while the flare examined above evolved over the course of several hours.

The shape and altitude change of the loops observed in this flare, as well as the observation of two different speeds for loops at different positions, are evidence that reconnection has taken place, and that the field lines are shrinking into a more relaxed state. This observation marks the first time, to our knowledge, that field line shrinkage has been observed on the disk in soft X-rays. Previous observations of shrinking loops by Švestka et al. (1987), Forbes & Acton (1996), and Hiei & Hundhausen (1996) were all seen in flares or coronal arches at or near the limb.

Since this flare is observed on the disk, there are potentially line-of-sight effects that distort the perceived geometry of the arch. For this flare, the intensity is fairly uniform along the arch, with the exception of a slight enhancement of the right-hand leg of the flare. Forbes & Acton (1996) studied the effects of different rotations on the measured intensity of a flare arcade, and they found that rotation of the top of the arcade toward the viewer, plus a rotation of the left side of the arcade toward the viewer, can produce an enhanced intensity in one leg of the arcade. This geometrical effect would cause us to underestimate the shrinkage percentage and velocity due to foreshortening effects. However, we believe this effect to be small, since Forbes & Acton (1996) found that rotation angles of 15° caused one loop leg to be dramatically brighter than the other, and the relative enhancement of the intensity in one loop leg is much less pronounced in the May 2 flare than it is in the Forbes & Acton (1996) simulations.

There could be explanations other than field line shrinkage for the apparent motion of the loops that we observe in the two flares. One possibility is that there are three-dimensional effects such as the "zipper" effect, which corresponds to features propagating along the line of sight when a flare is viewed on the limb.

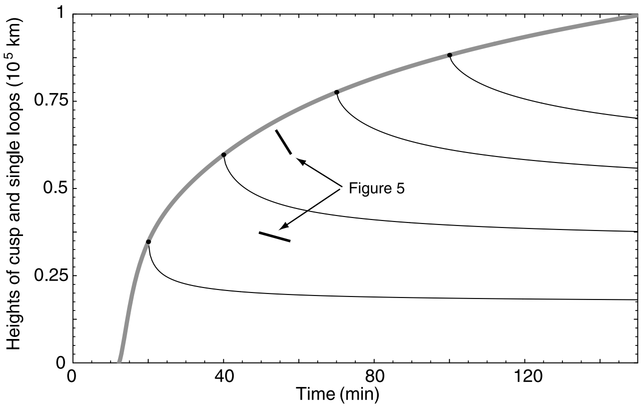

FIG. 7.—Heights of shrinking loops according to the model of Lin (2004). The thick gray curve is the height of the cusp. Circles indicate the time and altitude at which loops are formed, and the thin black curves trace the height of the loop, assuming a dipolar background field (see Lin 2004 for further details). The thick black line segments are the measured trajectories of shrinking loop tops from the 2007 May 2 flare, shown as white dotted lines in Fig. 5.

However, the zipper effect is primarily seen during the flare onset and impulsive phase, and both of our flare observations exhibit shrinkage well into the decay phase. The zipper effect further seems unlikely because we see the same shrinkage evolution both on the limb and in the disk. In the observations of the disk flare of 2007 May 2 in particular, it is clear that there is not a long arcade of flare loops, which is the usual morphology for flares that exhibit the zipper effect. A final argument against the zipper effect is that it would not account for the shape change observed in these events.

Another possibility is that the apparent shrinkage is caused by propagating thermal fronts. In fact, we do see a thermal front, but the front is the upward-moving bottom edge of the bright loop system. This behavior is due to the combination of the upward motion of the reconnection site and heating source together with the cooling of the heated plasma to a temperature below the filter threshold temperature. The downward-moving features are brighter than the surrounding loops, which suggests that they are denser and probably cooler than the surrounding plasma. It is hard to visualize how their apparent motion could be explained by a purely thermal process, as that would require some kind of heating or cooling mechanism operating counter to the heating and cooling processes of the overall loop system.

4. CONCLUSIONS

In this paper, we have presented observations of two flares that show evidence of field line shrinkage, one on the disk and one on the limb. These flares both have loops that change shape and bright loop structures that propagate downward as the flare progresses. For the flare of 2006 December 17, these features move at about 2–4 km s^{-1}. For the flare of 2007 May 2, we find that the brightest part of the loop structure shrinks at about 5 km s^{-1}, while fainter, higher loops shrink at a faster rate of about 45 km s^{-1}. We also track a compact loop top feature in this flare and find that it decreases in height quickly at first and more slowly later. These results agree well with theoretical predictions by Lin (2004) that a loop will shrink faster when it is closer to the reconnection site.

We measure the shrinkage of the December 17 flare to be about 27% over a 3.5 hr period, and that of the May 2 flare to be about 17% in 3 hr. These numbers are in the same range as those calculated in Forbes & Acton (1996) for similar flares observed with the SXT on *Yohkoh*.

The 2007 May 2 flare is particularly interesting because it is an observation of shrinkage on the disk of the Sun, and observations of this phenomenon were previously limited to the limb. The ability to resolve small-scale features in these flares and to track their motion is a direct consequence of the improved capabilities of the XRT, which are superior to those of previous instruments. These observations are now possible because the XRT has better spatial resolution, temporal resolution, and sensitivity than the SXT on *Yohkoh*, and the XRT can easily see the high-temperature plasma produced by reconnection.

The authors would like to thank the anonymous referee for insightful comments on the manuscript. *Hinode* is a Japanese mission developed and launched by ISAS/JAXA, with NAOJ as domestic partner and NASA and STFC (UK) as international partners. It is operated by these agencies in cooperation with ESA and the NSC (Norway). K. K. R. is supported by the NASA Solar-B Phase E contract to SAO, NNM07AA02C. D. B. S. and T. G. F. are supported by subcontract SV7-77002 from NASA/SAO to UNH.

REFERENCES

Feldman, U., Seely, J. F., Doschek, G. A., Strong, K. T., Acton, L. W., Uchida, Y., & Tsuneta, S. 1994, ApJ, 424, 444
Forbes, T. G. 1997, in ASP Conf. Ser. 111, Magnetic Reconnection in the Solar Atmosphere, ed. R. D. Bentley & J. T. Mariska (San Francisco: ASP), 259
Forbes, T. G., & Acton, L. W. 1996, ApJ, 459, 330
Forbes, T. G., & Malherbe, J. M. 1991, Sol. Phys., 135, 361
Golub, L., et al. 2007, Sol. Phys., 243, 63
Hiei, E., & Hundhausen, A. J. 1996, in IAU Colloq. 153, Magnetodynamic Phenomena in the Solar Atmosphere: Prototypes of Stellar Magnetic Activity, ed. Y. Uchida, T. Kosugi, & H. S. Hudson (Dordrecht: Kluwer), 125
Kano, R., et al. 2008, Sol. Phys., in press
Lin, J. 2004, Sol. Phys., 222, 115
Lin, J., Forbes, T. G., Priest, E. R., & Bungey, T. N. 1995, Sol. Phys., 159, 275
McTiernan, J. M., Kane, S. R., Loran, J. M., Lemen, J. R., Acton, L. W., Hara, H., Tsuneta, S., & Kosugi, T. 1993, ApJ, 416, L91
Priest, E. R., & Forbes, T. G. 2002, Astron. Astrophys. Rev., 10, 313
Reeves, K. K., Warren, H. P., & Forbes, T. G. 2007, ApJ, 668, 1210
Sui, L., & Holman, G. D. 2003, ApJ, 596, L251
Sui, L., Holman, G. D., & Dennis, B. R. 2004, ApJ, 612, 546
Švestka, Z. F., Fontenla, J. M., Machado, M. E., Martin, S. F., & Neidig, D. F. 1987, Sol. Phys., 108, 237
Tsuneta, S., Hara, H., Shimizu, T., Acton, L. W., Strong, K. T., Hudson, H. S., & Ogawara, Y. 1992, PASJ, 44, L63
Veronig, A. M., Karlický, M., Vršnak, B., Temmer, M., Magdalenić, J., Dennis, B. R., Otruba, W., & Pötzi, W. 2006, A&A, 446, 675
Vršnak, B., Temmer, M., Veronig, A., Karlický, M., & Lin, J. 2006, Sol. Phys., 234, 273